

A Single-Shot Method for Measuring the Energy Spectra of Pure Electron Plasmas Driven by $\mathbf{E} \times \mathbf{B}$ Rotation

Youngsoo PARK, Yukihiro SOGA, Masayuki SATO, Nozomi SUZUTANI¹⁾ and Takashi KIKUCHI¹⁾

Kanazawa University, Kanazawa 920-1192, Japan

¹⁾Nagaoka University of Technology, Nagaoka 940-2188, Japan

(Received 9 January 2019 / Accepted 29 January 2019)

In this study, a new single-shot method is developed for obtaining the parallel energy spectra of pure electron plasmas that rotate around the machine axis by the $\mathbf{E} \times \mathbf{B}$ drift. When the confinement voltage is raised to the ground level on a timescale that is comparable with the $\mathbf{E} \times \mathbf{B}$ rotation period, the electrons escape from the confinement region along the magnetic field lines over the potential barrier and onto a phosphor screen in the descending order of the energy of the electrons. This causes the phosphors to emit light at different points on the screen along the $\mathbf{E} \times \mathbf{B}$ rotation trajectory depending on the electron's energies. Further, the energy distribution can be derived from the luminosity distribution along this trajectory by appropriately converting these positions into their corresponding energy levels.

© 2019 The Japan Society of Plasma Science and Nuclear Fusion Research

Keywords: nonneutral plasma, $\mathbf{E} \times \mathbf{B}$ drift rotation, edge-dependent drift, parallel energy analysis

DOI: 10.1585/pfr.14.1201046

Eggleston's parallel energy analysis method for nonneutral plasmas confined in a Malmberg–Penning trap [1] is one of the most important experimental techniques for determining the energy distribution function (EDF) or temperature and is used in a diverse range of fields within nonneutral plasma physics, including two-dimensional vortex dynamics [2], beam physics [3], antimatter confinement [4] and even recent studies revealing energetic particles generation in ion plasmas [5, 6]. However, the Eggleston's method requires the target plasma to be sufficiently reproducible for determining the complete EDF because destructive measurement has to be repeatedly conducted to obtain data related to the escape of particles over different barrier potentials. Furthermore, it is difficult to uniquely determine the EDF without prior knowledge of the function's form (e.g., Maxwellian) because it is derived by differentiating discrete data (the cumulative number of escaped particles) with respect to the energy.

To address these issues, we have developed a method that can be directly determine the EDF from the results of a single-shot experiment on a pure electron plasma confined in a Malmberg–Penning trap [7], as depicted in Fig. 1. A target pure electron plasma with a peak density of $2 \times 10^{14} \text{ m}^{-3}$, a length of 230 mm and a $1/e^2$ width of 1.5 mm is rotated around the machine axis via $\mathbf{E} \times \mathbf{B}$ drift with a period of $t_{\mathbf{E} \times \mathbf{B}} = 40 \mu\text{s}$ in a uniform magnetic field of $B = 0.048 \text{ T}$. Figure 2 (a) depicts the plasma's cross-sectional electron number distribution (middle and bottom panels). To obtain this CCD image, we have conducted a conventional measurement by simultaneously dumping

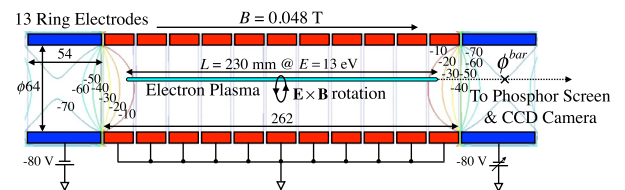


Fig. 1 Illustration of the $\mathbf{E} \times \mathbf{B}$ -rotating electron plasma in the trap (side view). Here, ϕ^{bar} is the lowest barrier voltage (creating the highest barrier potential energy $-e\phi^{bar}$) on a path along which the electrons can escape to the observation port.

all the electrons onto a phosphor screen by increasing the barrier voltage ϕ^{bar} (Fig. 1) from the confinement voltage of $\phi_0^{bar} = -69.1 \text{ V}$ to the ground level for a short period ($\Delta t_0 = 0.6 \mu\text{s}$), satisfying the condition $\Delta t_0 \ll t_{\mathbf{E} \times \mathbf{B}}$ (Fig. 2 (a), upper panel). When the Eggleston's method is applied to this $\mathbf{E} \times \mathbf{B}$ -rotating plasma, the measurement has to be repeated for many different barrier voltages manipulated at this high slew rate $d\phi^{bar}/dt$. In contrast, our single-shot energy spectrum measurement approach involved a slow adjustment of ϕ^{bar} in the same range over a period of $\Delta t_0 = 23 \mu\text{s} \sim t_{\mathbf{E} \times \mathbf{B}}$ (Fig. 2 (b), upper panel). Currently, only electrons with parallel energies E , which consist of kinetic energies and self-potential energies, satisfying the condition $E \geq -e\phi^{bar}$ could escape; further, the low-energy electrons initially remained confined, thereby undergoing additional $\mathbf{E} \times \mathbf{B}$ rotation. Therefore, the observed electron number, which is proportional to the luminosity, exhibited an elongated and energy-dependent spatial distribution that

author's e-mail: ysoga@staff.kanazawa-u.ac.jp

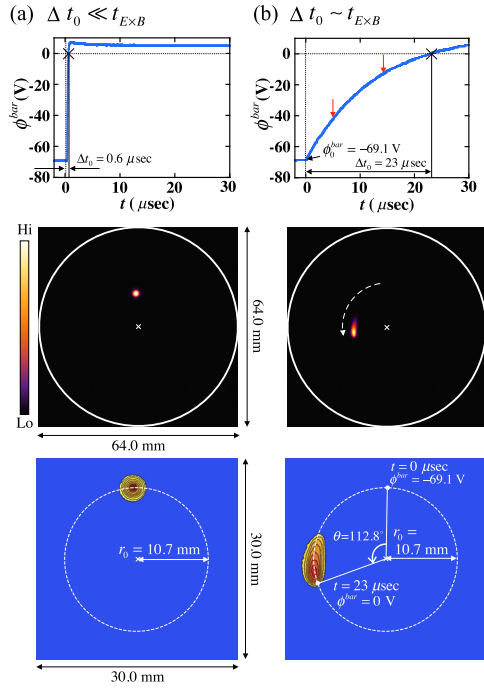


Fig. 2 Comparison between the experiments in which the electrons were simultaneously (a) and sequentially (b) dumped onto the phosphor screen, showing the luminosity distributions on the CCD images (middle panels) and enlarged contour maps (bottom panels) obtained while manipulating ϕ^{bar} as shown in the upper panels. Note that luminosity is proportional to the number of electrons.

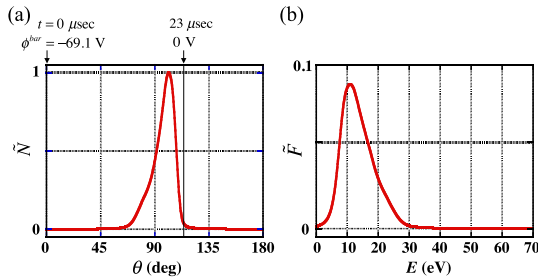


Fig. 3 (a) Normalized electron number distribution $\tilde{N}(\theta)$ observed along the $\mathbf{E} \times \mathbf{B}$ rotation trajectory shown in the bottom panel of Fig. 2 (b). (b) Normalized energy spectrum $\tilde{F}(E)$ derived from $\tilde{N}(\theta)$.

followed the $\mathbf{E} \times \mathbf{B}$ rotation trajectory (Fig. 2 (b), middle and bottom panels). Figure 3 (a) plots the normalized electron number $\tilde{N}(\theta)$ as a function of the angle θ along the trajectory of the plasma's center. The major advantage of our approach is that this single spatial distribution measurement reflects the entire energy distribution.

Figure 3 (b) shows the EDF $\tilde{F}(E)$, derived from $\tilde{N}(\theta)$ by converting the observed angle θ into the associated barrier potential energy E . To calculate this, we adopt the following iterative approach. First, we approximate the remaining electron's angular velocity $\omega(\phi^{bar})$ by a suitable decreasing function that satisfies the conditions $\omega(\phi_0^{bar}) =$

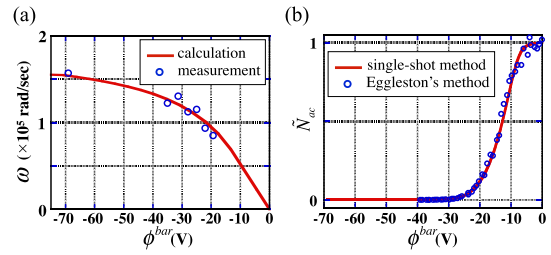


Fig. 4 Dependence of the $\mathbf{E} \times \mathbf{B}$ drift angular velocity (a) and normalized cumulative number of electrons detected (b) on the barrier voltage ϕ^{bar} .

ω_0 and $\omega(0) = 0$. Here, ω_0 is the angular velocity at the confinement voltage ϕ_0^{bar} , which can easily be obtained via the nondestructive measurement of the image current [8], as indicated by the leftmost point in Fig. 4 (a). Second, we obtain the observed angle θ , corresponding to the position of the remaining electrons, as a function of ϕ^{bar} by integrating $\omega(\phi^{bar})$ from ϕ_0^{bar} to ϕ^{bar} , as follows:

$$\theta(\phi^{bar}) = \int_{\phi_0^{bar}}^{\phi^{bar}} \frac{\omega(\phi^{bar'})}{d\phi^{bar'}/dt} d\phi^{bar'}. \quad (1)$$

Here, the slow rate $d\phi^{bar}/dt$ is calculated numerically based on the measured $\phi^{bar}(t)$ (Fig. 2 (b), upper panel). Third, we convert the observed $\tilde{N}(\theta)$ into $\tilde{N}(\phi^{bar})$ using (1), then calculate $\tilde{F}(E)$ by applying the relation $E = -e\phi^{bar}$ to $\tilde{N}(\phi^{bar})$. Fourth, we update $\omega(\phi^{bar})$ by taking the ensemble average of the radial electric field acting on the electrons at the radial position r_0 , as follows:

$$\omega(\phi^{bar}) = \frac{1}{r_0 B} \int_0^{-e\phi^{bar}} \tilde{F}(E) (\overline{E_r^{ext}} + E_r^{im}) dE, \quad (2)$$

where $\overline{E_r^{ext}}$ is the effective electric field due to the trap potential and E_r^{im} is the electric field due to the image charge induced on the conducting wall [9]. Finally, we obtain self-consistent solutions for $\omega(\phi^{bar})$ and $\tilde{F}(E)$ by repeating steps from two to four until successive iterations produce the same distributions for $\omega(\phi^{bar})$ and $\tilde{F}(E)$.

Figure 4 (a) compares our calculated $\omega(\phi^{bar})$ values with the measured data, showing that they are in good agreement. Here, the measured data except for the left most point are approximately estimated from the positions of the peak luminosities observed from the experiments conducted by increasing ϕ^{bar} to different values in the range between the two red arrows denoted in the upper panel of Fig. 2 (b). To directly compare our single-shot approach with the Eggleston's method, we have calculated the cumulative number of escaping electrons \tilde{N}_{ac} by integrating the $\tilde{F}(E)$ spectrum in Fig. 3 (b). Figure 4 (b) denotes that the resulting \tilde{N}_{ac} values are very close to the data obtained via the Eggleston's method, which required more than 40 experimental runs, clearly demonstrating both the validity and the convenience of our single-shot measurement technique.

This work was supported by JSPS KAKENHI Grant Number JP17K05724.

- [1] D.L. Eggleston, C.F. Driscoll, B.R. Beck, A.W. Hyatt and J.H. Malmberg, *Phys. Fluids B* **4**, 3432 (1992).
- [2] A.J. Peurrung and J. Fajans, *Phys. Fluids B* **5**, 12 (1993).
- [3] R.C. Davidson, *Physics of Nonneutral Plasmas* (Addison-Wesley, Redwood City, 1990) p.539.
- [4] G.B. Andresen *et al.*, *Nature* **468**, 673 (2010).
- [5] H. Himura, S. Kawai, K. Akaike, S. Okada, J. Aoki and S. Masamune, *Phys. Plasmas* **24**, 102129 (2017).
- [6] K. Akaike and H. Himura, *Phys. Plasmas* **25**, 122108 (2018).
- [7] Y. Kiwamoto, K. Ito, A. Sanpei and A. Mohri, *Phys. Rev. Lett.* **85**, 3173 (2000).
- [8] K. Ito, Y. Kiwamoto and A. Sanpei, *Jpn. J. Appl. Phys.* **40**, 2258 (2001).
- [9] Y. Soga, T. Mimura, Y. Kato and Y. Park, *Plasma Fusion Res.* **8**, 2401034 (2013).